

We are IntechOpen, the world's leading publisher of Open Access books Built by scientists, for scientists

6,900

Open access books available

186,000

International authors and editors

200M

Downloads

Our authors are among the

154

Countries delivered to

TOP 1%

most cited scientists

12.2%

Contributors from top 500 universities



WEB OF SCIENCE™

Selection of our books indexed in the Book Citation Index
in Web of Science™ Core Collection (BKCI)

Interested in publishing with us?
Contact book.department@intechopen.com

Numbers displayed above are based on latest data collected.
For more information visit www.intechopen.com



Models of Biomimetic Tissues for Vascular Grafts

Mihai Chirita¹ and Clara Ionescu²

¹University of Medicine and Pharmacy, Faculty of Biomedical Engineering, Iasi

²Ghent University, Electrical energy, Systems and Automation, Gent-Zwijnaarde

¹Romania

²Belgium

1. Introduction

The symbiosis between the terms nature (plants, animals) and engineering has gained a large interest from the bioengineering research community (Bronzino, 2006). The concept is based on the idea that life has simple and effective rules to provide the highest efficiency with minimal requirements for energy resources and food supply. The result is a diversity of biomimetic systems, serving either biological replacements of tissue or organs (e.g. tissue engineering, artificial and bio-artificial organs), either purely technological process (e.g. swarm control, unmanned aerial vehicles, water and aerial vehicles, etc) (Cohen, 2006; Chirita, 2009).

The future of medicine is no longer ignorant to the adaptability of life forms to various environmental conditions and to various purposes, but it integrates these aspects as part of the intrinsic process of efficient evolution. Nowadays, biomaterials are becoming a *de facto* element in orthopaedic implants, regenerative tissues, cardiovascular stents, cardiac valves, pacemakers, tissue replacements, nano-robotics, haptic surgical devices, biosensors, nano-medicine, etc (Archer and Ralphs, 2010).

Recently, the term of *biomaterials* is usually paired with that of *future medicine* (see figure 1). The last decennia has marked the era of biomaterials and artificial tissues for implants, regenerative materials, cardiovascular stents, pacemakers, nanorobotics, biosensors, etc. In fact, the bionic medicine refers to a replacement or an enhancement in the efficiency of a biological function by mechanical devices. The bionic implants should not be confounded with medical prosthesis, since they really copy the biological function to its perfection, while striving to improve it. Within the healthcare paradigm, there is an intensive research activity in biomedical engineering, biotechnology and bioelectronics. As such, the science of implant medicine, implantology, is undergoing a significant transformation, originated by the conceptual change from classical forms of implants (mechanical, etc) to that of biomimetic implant. The advantages of these biomimetic implants are mainly post-surgical, reducing the healing time interval in some cases (i.e. bone, skin, blood vessels, cardiac valves). The principles of biomimetics employ the medical and biological knowledge to the point of becoming natural elements in tissue engineering and tissue remodelling processes.

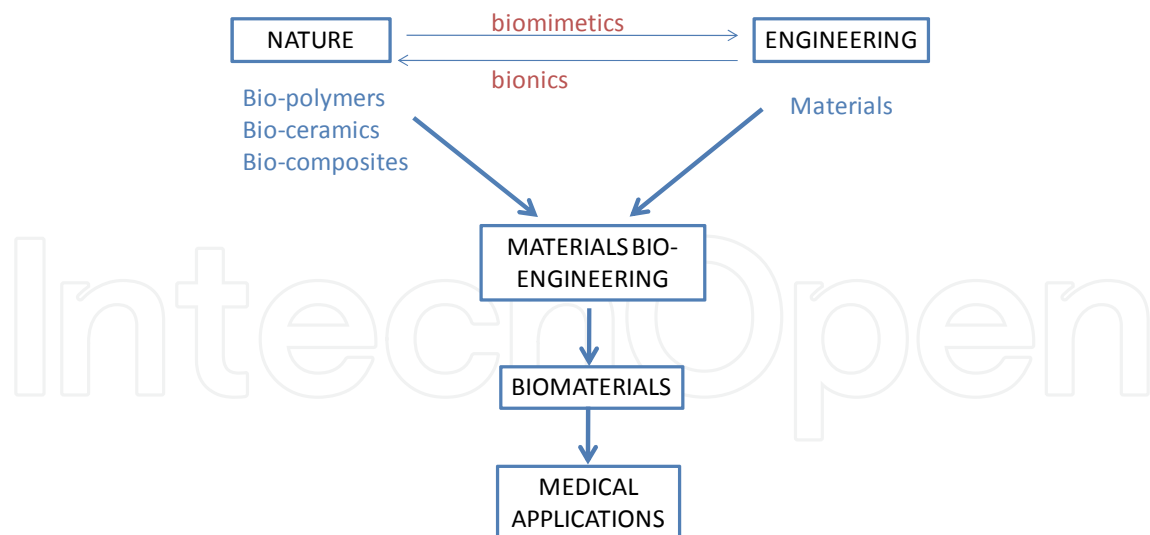


Fig. 1. Schematic representation of the interaction between the different concepts of the interaction between nature and engineering.

By copying ideas from nature and by implementing these simple yet effective procedures, the quality of a manifold of engineering processes can be increased significantly. However, the general problem of bioengineers remains the same: the manufacturing costs and healthcare risks. By definition, nature offers intrinsic solutions, produced by a natural chain of bio-chemical interactions. Hence, the regulation of all biological processes is more efficient in the nature than in an artificial framework. The biological feedback remain a key element in the maintenance of this intrinsic efficiency that nature performs on all living organisms. The intrinsic property of these natural materials with specific material properties and dynamic performance, is that of a highly-optimized, strictly defined structure and inter-relation of these structures to form living organisms.

Biopolymers are polymers produced by living organisms. Cellulose, starch, chitin, proteins, peptides, DNA and RNA are all examples of biopolymers, in which the monomeric units, respectively, are sugars, amino acids, and nucleotides. Chitin is a macromolecule found in the shells of crabs, lobsters, shrimps and insects. Chitin can be degraded by chitinase. Chitin fibers have been utilized for making artificial skin and absorbable sutures (Chirita, 2008). Chitin is insoluble in its native form but chitosan, the partly deacetylated form, is water soluble. The materials are biocompatible and have antimicrobial activities as well as the ability to absorb heavy metal ions. They also find applications in the cosmetic industry because of their water-retaining and moisturizing properties. Using chitin and chitosan as carriers, a water-soluble prodrug has been synthesized. Modified chitosans have been prepared with various chemical and biological properties (Chirita, 2001). Optical microscopy shows that those films that contain a lower amount of calcium and a higher content of silica are more uniform in appearance (Ionescu and Chirita, 2008). Collagen and elastin are extracellular matrix structural proteins that are important stress-bearing constituents of tissues. These fibers differ significantly in their mechanical properties, with collagen being three to four orders of magnitude stiffer than elastin. The advantages of using collagen products in medicine are its very low antigenicity, excellent histocompatibility, ease of association with other biologically active species such as glycosaminoglycans, and its polyelectrolytic behavior. The reconstitution of collagen from solution into native fibers is also of interest because of its regenerative applications (Archer and Ralph, 2010; Hariton *et al*, 2007). For example, the

fibroin produced by the silk worms (*Bombix Mori*), respectively the dragline produces by a kind of spider (*Nephila Clavipes*) are two examples of fibroid polymer which pose intrinsic resistance, elasticity and biocompatibility.

Another important aspect is that of structural optimization. Hierarchical structures are by definition a complex of micro- and macro-molecules, inter-woven by similar structures. This leads to the concept of multi-level hierarchies, which pose specific properties. In the case of wood cellulose, or cartilage collagen, the specific multi-level structure offers a manifold of applications (biomaterial properties). Within the process of natural growth, the biomaterial properties are of crucial importance, since they can lead to soft or hard tissue consistency. Nowadays, the progress in tissular replacement engineering has enabled the combination of biomaterials with regenerative characteristics, allowing the tissue to grow and interact with the natural tissue. Hitherto, the artificial materials (biomaterials) have not yet become as proficient as the natural materials, but efforts are being made in the field of vascular grafts (Chirita, 2009).

Many studies have been undertaken to develop acceptable small diameter vascular prostheses. Detailed knowledge of the mechanical properties of the arterial wall is crucial for understanding the changes which occur in the vascular system in case of arteriosclerosis and aneurysm disease. The atherosclerosis is the essential characteristic of pathologies pressure causing diseases at the arterial level (e.g. plaque rupture, myocardial infarction, death ischemic). Hence, it is crucial to obtain constitutive equations that describe the mechanical properties of native tissues which can be used for diagnostic purposes (Mandru *et al*, 2009). The tissue growth, the blood clotting and the affecting blood elements are influenced by surface energy. Hence, the additional knowledge of the static contact angle, free surface energy, the interfacial tension and the critical superficial tension become essential for the purpose of medical replacements.

In this paper we present an overview of parametric models for the stress-strain relationship in artificial tissues for vascular replacements. Their values are compared to those of native tissues. The paper provides contributions in modeling aspects and in experimental analysis. The models and indexes presented in this chapter will help researchers gather insight into the required properties for restoration and hemo-compatibility of the native tissue and their relation to the desired properties in the synthetic tissues. As such, these properties are crucial in the improvement of natural inclusion, tissue compatibility and growth.

2. Materials and measurement protocol

The samples for native tissue assessment have been prevailed from three pigs, as presented in (Mandru *et al*, 2009). A biometric description of the sampled tissues is given in Table 1, *i.e.* 6 samples from the carotid and 2 samples from the thoracic arteries.

Sample	Longitudinal length (mm)	Transversal length (mm)	Longitudinal width (mm)	Transversal width (mm)	Thickness (mm)
Carotid artery	50	-	11	-	0.938
Thoracic artery	30	30	6.78	7.38	1.43

Table 1. Biometric values for the sampled tissues.

The traction device depicted by figure 2 consists of a framework capable of bearing the major strengths, a fixed wooden plate, as well as a system able to apply the various testing force values.

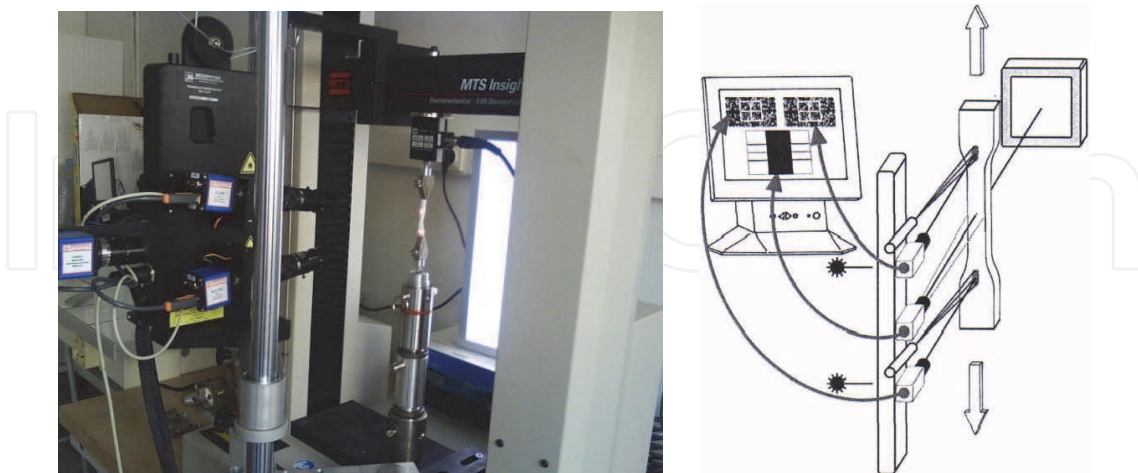


Fig. 2. Traction device and its corresponding schematic overview.

The device is scheduled to pull the two extremes of the sample tested at a constant speed and to register continuous and simultaneous the strain of the sample. The system contains: *i*) a complete Laser Speckle - extensometer which measures axial and transverse deformation simultaneously, and *ii*) a traction device that creates the necessary framework in order to obtain variation in strain. The Laser Speckle extensometer is connected to a PC video processor that measures the movement of the two modes via two video-cameras in a master-slave configuration. The recorded result is thus the axial deformation of the tested sample.

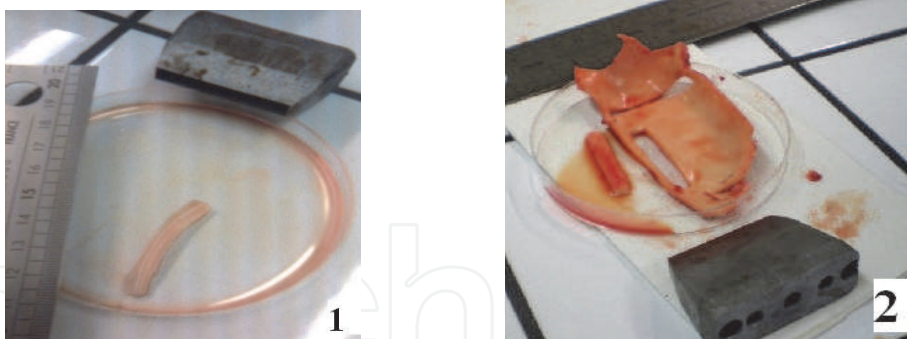


Fig. 3. Example of samples from the carotide (1) and the toracic (2) arteries prevailed from the pig.

Figure 3 depicts the materials, cut in rectangular shapes with a custom-designed die of various sizes: 30 or 50 mm. The thicknesses of the tissue samples were determined in cross-sections by aid of optical microscopy. After the shape and dimension of the sample was determined, the sample was attached to the test-frame of the traction device, while fixed at its cephalic and caudal ends by using a custom-designed gripping device, specially developed to prevent slippage. The gripping device consisted of two opposing metal blocks fastened together to fix the inferior and superior ends. The measured stress-strain relationship are depicted in figure 4, for the longitudinal carotid artery, longitudinal and transversal thoracic aorta.

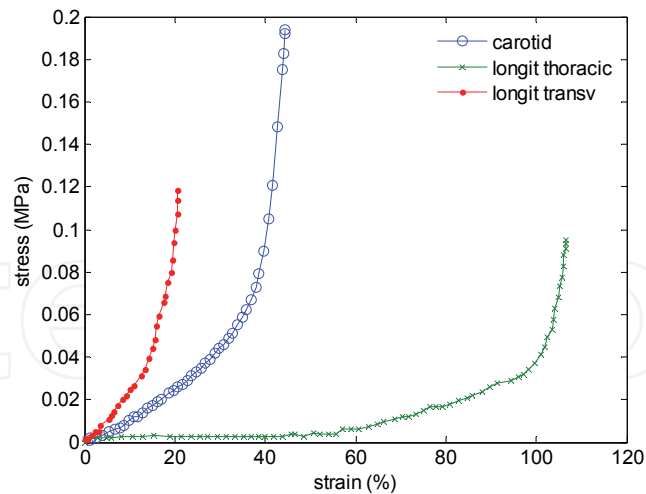


Fig. 4. Stress-strain curves for the transversal thoracic aorta, the longitudinal thoracic aorta and the longitudinal carotid artery.

2. Parametric modelling

The parametric models presented in this chapter are based on power law modelling principles (Gao *et al.*, 2007). These are compared to polynomial models, which are basic tools for data analysis (Ljung, 1999). For the first type of models, the corresponding energy feature was calculated using the Abaques® software platform. Since the modules of elasticity are not the most appropriate parameters to describe the arterial wall subjected to different deformation, the suggested models characterizing the features of energy seem to deliver more insight in the mechanical properties of the materials. Using the relation:

$$W = \sum_{i=1}^N C_{i0} (I_1 - 3)^i + \sum_{i=1}^N \frac{1}{D_i (J^{el} - 1)^{2i}} \quad (1)$$

with W the energy function, N the total number of measurements, I_1 is the first strain invariant and J is the volumetric strain (Pena *et al.*, 2006; Zidi and Cheref, 2003). As a result of fitting (1) to the measured energy-strain curves, one obtains a polynomial relation from the Abaques® software platform. For the comparison purpose, a power law model structure has been applied to fit the stress-strain curves:

$$\sigma = A_1 \varepsilon^{\gamma_1} + B_1 \quad (2)$$

where σ denotes the stress (MPa), ε denotes the strain (%) and A (MPa), γ_1 (-), B_1 (MPa) are identified constants. The stress σ is defined by the measured tension divided by the resting cross-sectional area of the strips and the strain ε is the axial tissue strain, defined as $\varepsilon = (L - L_{rest}) * 100 / L_{rest}$, where L is the length as a result of the applied tension and L_{rest} is the length of the strip at rest. The modelling errors can be further reduced by optimizing the model structure. In viscoelastic materials, it is known that collagen fibers are triggered after the elastin fibers, which may suggest that two separate traction phenomena could be deduced if two power law parameters are introduced in the model:

$$\sigma = A_2 \varepsilon^{-\gamma_2} + C \varepsilon^{-\eta} + B_2 \quad (3)$$

with σ the stress (MPa) and ε the strain (%) input to the model and $A_2, B_2, \gamma_2, C, \eta$ fitted variables. Additionally, the molecular weight of the polymer of interest is known to affect its creep behavior. The effect of increasing molecular weight tends to promote secondary bonding between polymer chains and thus make the polymer more creep resistant, which is important from biomimetic point of view (Bronzino, 2006). Another possibility is to assume an exponential function in terms of the strain, which relates to the intrinsic creep:

$$\sigma = A_3 \varepsilon^{-\gamma_3} + D e^{\lambda \varepsilon} \quad (4)$$

with σ the stress (MPa) and ε the strain (%) input to the model and $A_3, \gamma_3, D, \lambda$ fitted coefficients.

The model parameters were estimated using a nonlinear least square optimization algorithm, making use of the MatLab® function LSQNONLIN. The optimization algorithm is a subspace trust region method and is based on the interior-reflective Newton method described in (Coleman and Li, 1996). The large-scale method for LSQNONLIN requires that the number of equations (i.e. the number of elements of cost function) must be at least as large as the number of variables. The large-scale method for lsqnonlin requires that the number of equations (i.e., the number of elements of cost function) be at least as great as the number of variables. The iteration involves the approximate solution using the method of preconditioned conjugate gradients, for lower and upper bounds. In this application, the lower bounds were set to 0 (parameters cannot have negative values) with no upper bounds. The optimization stopped when a termination tolerance value of $10e^{-8}$ was achieved. In all cases we obtained a correlation coefficient between data and model estimates above 80% (Ljung, 1999). In order to assess the performance of each model, the relative and absolute error values were calculated as with M the measured values and \hat{M} the estimated values for the model output:

$$E_{abs} = \frac{1}{N} \sum_{i=1}^N |\hat{M}_i - M_i|, \quad E_{rel} = \frac{1}{N} \sum_{i=1}^N \frac{|\hat{M}_i - M_i|}{|M_i|} \times 100(\%) \quad (5)$$

with M the measured values, \hat{M} the estimated values for the model output and N the total number of data samples. The residual norm was also calculated as:

$$RN = \|F(x)\|_2^2 \quad (6)$$

with $F(x)$ the evaluated output for the identified parameter vector x .

3. Results and discussion

The energy feature for carotid and thoracic artery using (1) was optimally captured by a 5th and a 6th order polynomial, respectively. The identified polynomial coefficients are given in Table 2, in which C_1 and C_2 are the neo-hook= $\mu/2$ constants of the rigidity module, C_3 scales the exponential stress, C_4 is related to the rate of un-crimping collagen, C_5 is the elastic modulus of the straightened collagen fibers, D is the inverse of the bulk modulus: $k=1/D$, $k=3\mu/2\mu$, with k the coefficient of stiffness compression.

For the power-law model coefficients, the values are given in Table 3. The corresponding modeling errors are given in Table 4. Although the polynomial representation offers minimal modeling errors, it has the dis-advantage of high number of parameters to be

identified. On the other hand, at the expense of somewhat higher modeling errors, the power-law model from (2) has only three parameters to be identified. The identified model parameters are given in tables 3-4-5, along with the corresponding modelling errors, for the models (2), (3) and (4) respectively. For all models, the native data samples were $N=47$ for carotid artery, $N=71$ for longitudinal thoracic aorta and $N=32$ for transversal thoracic aorta.

Sample	C_1	C_2	C_3	C_4	C_5	C_6	D
carotid artery	0.014	0.072	0.12	0.125	0.602	-	0,000
longitudinal thoracic artery	0.029	0.070	0.011	-1.53	3.741	3.040	0,000

Table 2. The identified coefficients of the polynomial (1) for the hiperelastic material.

Sample	A_1	B_1	γ_1	E_{abs}	E_{rel}	RN
carotid	1.54×10^{-6}	0.0038	-3.0339	0.0100	0.3394	0.0089
longit th	3.44×10^{-6}	0.0113	-3.0080	0.0074	0.3481	0.0090
transv th	11.7×10^{-6}	0.0073	-2.9889	0.0036	0.4959	0.0006

Table 3. The identified coefficients of the power-law model (2).

Sample	A_2	B_2	γ_2	C	η	E_{abs}	E_{rel}	RN
carotid	3.30×10^{-8}	-0.0273	-4.1075	0.0329	0.0497	0.0079	0.4252	0.0050
longit th	6.10×10^{-8}	-0.0425	-4.1273	0.0440	0.1369	0.0053	0.1570	0.0047
transv th	42.7×10^{-8}	-0.0643	-4.0418	0.0695	0.0659	0.0028	0.3507	0.0003

Table 4. The identified coefficients of the enhanced power-law model (3).

Sample	A_3	γ_3	D	λ	E_{abs}	E_{rel}	RN
carotide	0.0044	-0.5099	100×10^{-6}	0.1726	0.0041	0.3846	0.0011
longit th	0.0034	-0.7923	4×10^{-5}	0.2299	0.0022	0.1153	0.0006
transv th	-0.0032	0.0593	6000×10^{-6}	0.1411	0.0024	0.1558	0.0003

Table 5. The identified coefficients of the combined power-law and creep model (4).

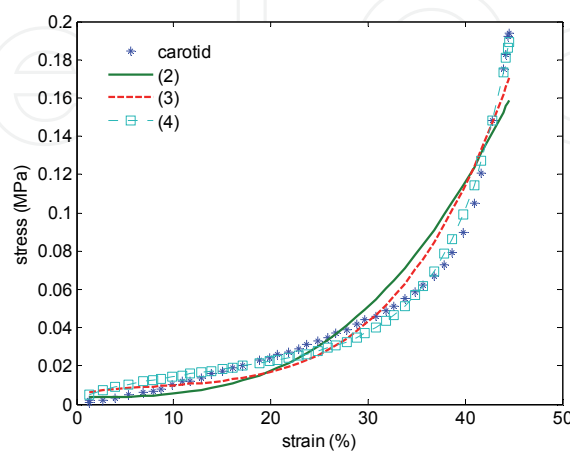


Fig. 5. Evaluation of stress-strain curves for models (2)-(3)-(4) on the experimental data provided from the carotid artery.

From figures 5-7 one may conclude that all models capture reasonably well the experimental data. Notice that the identification was not subject to any physiological constraints, since no reference data was available a priori. The model from (2) was clearly outperformed by model (3), while model (4) could not reduce the modelling errors in a significant manner. The residual norm seemed to give most stable trend of error decrease as model complexity increases. All models seemed to best capture properties in the transversal thoracic aorta, perhaps due to a stronger nonlinear behavior. This suggests that non-constitutive models (i.e. lumped models) can prevalently describe native tissues with higher nonlinearity, without increasing significantly the numerical complexity of the model structure.

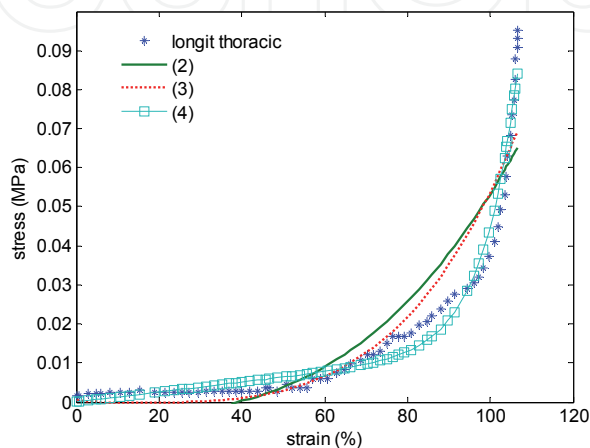


Fig. 6. Evaluation of stress-strain curves for models (2)-(3)-(4) on the experimental data provided from the longitudinal thoracic aorta.

For all three sets of data, the two parts of the model from (4): $A_3\varepsilon^{-\gamma_3}$ and $De^{\lambda \cdot \varepsilon}$ have different contribution related to two stress segments. In the first part, for ε between 20% and 40%, the first part has a major contribution to stress σ . For higher strains, the contribution of the first term becomes negligible and the second term become the major contribution to the total stress. The point when the contribution of the two factors are balanced is however not precisely determined, and varies for different types of the blood vessels (Bronzino, 2006).

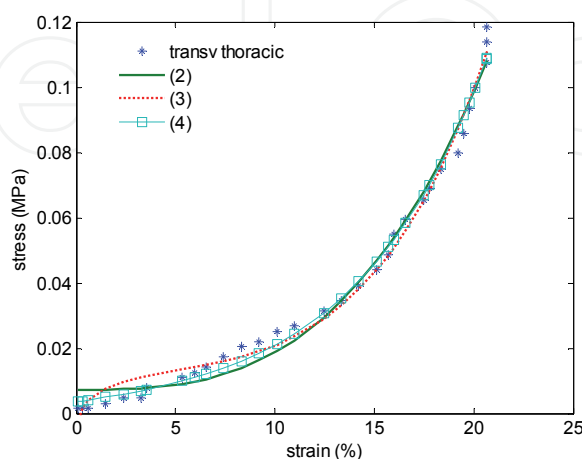


Fig. 7. Evaluation of stress-strain curves for models (2)-(3)-(4) on the experimental data provided from the transversal thoracic aorta.

The variations in the magnitude of the model parameters can be related to variations in the data input (strain). A possible origin for the high variations in the first model parameter is that for lower strains, the power-law has smaller variations for higher values of parameters (saturation for strain variations with respect to variations in the model parameter). After a threshold value, the power law which takes into account both collagen and elastin distribution becomes less important with respect to the exponential term. It is difficult to compare our identified model parameters with data from literature, due to a lack of available information. To the authors knowledge, such lumped models do not exist in the literature on the respective native tissue.

In similar studies on dog arteries, deformations were computed using the dimensions of the unloaded free-floating vessel segment as a reference value (Dobrin, 1999). Blood vessels adapt morphologically and mechanically to increased wall stress. Some authors suggest that deformations should not be computed with respect to the retracted, unloaded state because the vessels never exist in vivo at these dimensions. Moreover, when fully unloaded, the vessels manifest evidence of residual stresses, ie, residual compression near the intima and residual tension near the outer margin of the media (Fung, 1990). As a result, when a ring of artery is transected, it springs open to assume a larger radius. All of these observations imply a highly integrated, interlocked anatomic system of elastin and vascular muscle where one element, elastin, cannot be extended without extending the other, i.e. the attached vascular muscle cells. Enzymatic degradation studies in vitro and physiological analysis in vivo suggest that the collagen fibers are loose, without substantially load-bearing at low and physiological pressures (Fung, 1990). These observations, coupled with observed uniformity of response of the elastic lamellae across the wall suggest that the artery wall behaves mechanically as though it were a homogeneous material, despite its marked histologic heterogeneity (Dobrin, 1999; Fung, 1990).

4. Conclusion

This chapter provides an overview of available tools and several parametric models to characterize the mechanical properties in both native and artificial tissues. A manifold of native tissue samples are analyzed and characterized. A novel concept has been presented for determining the mechanical properties of native and biomimetically formed arterial tissue using data from the energy function. The results have been found to be dependent on the surrounding environment, the existence of preconditioning, the static and dynamic experiments, e.g. the length of tissue specimen, the type of load, the loading speed, the sampled surface, the values and intervals of load variations, the residual strains, etc. The mechanical properties of the tissues may also depend on the status of the donor, as well as the conservation conditions of native tissues.

Furthermore, we presented alternative lumped models for stress-strain relationships in native tissues, capturing well the intrinsic properties.

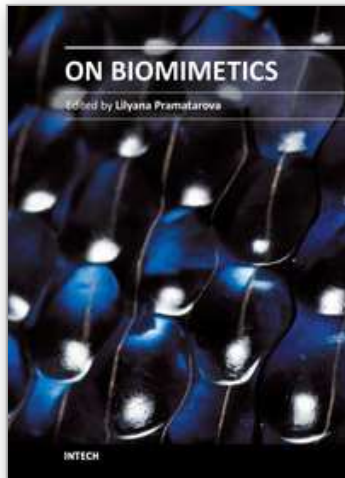
5. Acknowledgements

This paper represent a part of un graduation work and is realized with the help of an Erasmus student mobility at the Higher Institute of Bio-Science, University Paris 12, France, based on a bilateral agreement with the Faculty of Medical Bio-Engineering, Iasi, Romania. The results presented in this paper are also realized in collaboration with the Research

Institute „Petru Poni”, Departement of Polyadditon, Iasi, Romania. The authors acknowledge the technical support from the members of Surgical Center Henri Mondor, University Paris 12, France, and from the Research Institute „Petru Poni”, Departement of Polyadditon, Iasi, Romania.

6. References

- Archer C., Ralphs J., (2010) *“Regenerative medicine and biomaterials for the repair of connective tissues”*, CRC Press, ISBN 9781439801109
- Bronzino J., (2006) *“Biomedical Engineering Handbook”*, 3rd edition, CRC Press, ISBN 9780849321245
- Coleman T.F., Li Y., (1996) „An interior trust region approach for nonlinear minimization subject to bounds”, *SIAM Journal on Optimization*, 6, 418-445.
- Cohen Y.B. (2006). *Biomimetics: biologically inspired technologies*, CRC Taylor & Francis, ISBN 978-084-933-163-3
- Chirita, M. (2001) *Biopolymers and natural composites*, Colectia Bioinginerie Medicala (in Romanian), Nr.1, Ed.Tehnica-Info, Chisinau, Moldova Republic
- Chirita, M. (2009) *Treatise on Biomolecules, Vol.1&2*, Ed.SEDCOM LIBRIS, Iasi, Romania
- Chirita, M., (2008), “Mechanical properties of collagen biomimetic films formed in the presence of calcium, silica and chitosan”, *Journal of Bionics Engineering*, 5(2), 149-159
- Dobrin P. (1999) “Distribution of lamellar deformations”, *Hypertension*, 33, 806-810
- Fung F. (1990) „Stress, strain, and stability of organs”. In: *Biomechanics, Motion, Flow, and Growth*. New York, NY: Springer-Verlag; 382-451
- Gao J., Cao Y., Tung W., Hu T., (2007), “Multiscale analysis of complex systems”, Wiley Press, ISBN 978-0-471-65470-4
- Hariton I., DeBotton G., Gasser T., Holzapel G., (2007), “Stress-modulated collagen fiber remodeling in a human carotid bifurcation”, *Journal of theoretical Biology*, 248, 460-470.
- Ionescu C., Chirita M., (2008) "Stress-strain properties of natural and biomimetical formed collagen constructs", *Int J of Technology and Healthcare*, IOS Press, 16(6), 437-444
- Ljung L., (1999) *“System Identification: theory for the user”*, IEEE Press
- Mandru M., Ionescu C., Chirita M., (2009) Modelling mechanical properties in native and biomimetically formed vascular grafts, *Journal of Bionic Engineering*, 6(4), 371-377
- Pena E., Martinez M., Calvo B., Doblare M., (2006) „On the numerical treatment of initial strains in biological soft tissues”, *Int. Journal of Numerical Methods in Engineering*, 68, 836-860
- Zidi M., Cheref M., (2003), „Mechanical analysis of a prototype of a small diameter vascular prosthesis. Numerical simulation”, *Computers in Biology and Medicine*, 1, 1-11



On Biomimetics

Edited by Dr. Lilyana Pramatarova

ISBN 978-953-307-271-5

Hard cover, 642 pages

Publisher InTech

Published online 29, August, 2011

Published in print edition August, 2011

Bio-mimicry is fundamental idea –How to mimic the Nature™ by various methodologies as well as new ideas or suggestions on the creation of novel materials and functions. This book comprises seven sections on various perspectives of bio-mimicry in our life; Section 1 gives an overview of modeling of biomimetic materials; Section 2 presents a processing and design of biomaterials; Section 3 presents various aspects of design and application of biomimetic polymers and composites are discussed; Section 4 presents a general characterization of biomaterials; Section 5 proposes new examples for biomimetic systems; Section 6 summarizes chapters, concerning cells behavior through mimicry; Section 7 presents various applications of biomimetic materials are presented. Aimed at physicists, chemists and biologists interested in biomineralization, biochemistry, kinetics, solution chemistry. This book is also relevant to engineers and doctors interested in research and construction of biomimetic systems.

How to reference

In order to correctly reference this scholarly work, feel free to copy and paste the following:

Mihai Chirita and Clara Ionescu (2011). Models of Biomimetic Tissues for Vascular Grafts, On Biomimetics, Dr. Lilyana Pramatarova (Ed.), ISBN: 978-953-307-271-5, InTech, Available from:

<http://www.intechopen.com/books/on-biomimetics/models-of-biomimetic-tissues-for-vascular-grafts>

INTECH
open science | open minds

InTech Europe

University Campus STeP Ri
Slavka Krautzeka 83/A
51000 Rijeka, Croatia
Phone: +385 (51) 770 447
Fax: +385 (51) 686 166
www.intechopen.com

InTech China

Unit 405, Office Block, Hotel Equatorial Shanghai
No.65, Yan An Road (West), Shanghai, 200040, China
中国上海市延安西路65号上海国际贵都大饭店办公楼405单元
Phone: +86-21-62489820
Fax: +86-21-62489821

© 2011 The Author(s). Licensee IntechOpen. This chapter is distributed under the terms of the [Creative Commons Attribution-NonCommercial-ShareAlike-3.0 License](#), which permits use, distribution and reproduction for non-commercial purposes, provided the original is properly cited and derivative works building on this content are distributed under the same license.

IntechOpen

IntechOpen